ELSEVIER

Marine Geology 165 (2000) 87–108

MARINE GEOLOGY
INTERNATIONAL JOURNAL OF MARINE GEOLOGY, GEOCHEMISTRY AND GEOPHYSICS

www.elsevier.nl/locate/margeo

Stratigraphy and Holocene evolution of a regressive barrier in south Brazil

G.C. Lessa[a,*], R.J. Angulo[b], P.C. Giannini[c], A.D. Araújo[b]

[a]*Centro de Estudos do Mar-Universidade Federal do Paraná, Pontal do Sul (PR), Brazil*
[b]*Departamento de Geologia, UFPR, C.P. 19011, Curitiba (PR) 81531-990, Brazil*
[c]*Instituto de Geociências-USP, Rua do Lago 562, Cidade Universitária, São Paulo (SP) 05508-900, Brazil*

Received 17 June 1998; accepted 7 October 1999

Abstract

The Paranaguá coastal plain is a 600 km^2 barrier system located in south Brazil (25° 30′ S) and is largely made up of Pleistocene and Holocene beach ridges. Sea level history in the area is characterized by a gradual, 3.5 m sea level fall in the last 5000 years. Several reverse-circulation drill logs from the Pleistocene and Holocene sectors allowed for the definition of a general morphostratigraphic model of the coastal plain, which proposes the staking of at least two generations of marine deposits upon continental and paleo-estuarine sediments. Analysis of shallow vibro-cores and exposures along back-barrier creeks indicates the existence of four transgressive (estuarine, estuarine channel, overwash and flood-tidal delta) and three regressive (beachface, nearshore and upper shoreface) sedimentary facies in the Holocene section of the coastal plain. The morphostratigraphy suggests that barrier emplacement took place at the last stages of the post-glacial marine transgression, when the back-barrier estuary was squeezed in between the Pleistocene and Holocene barriers. Holocene barrier progradation was significant in both the shore-normal and longshore direction, and was apparently very swift in the last thousand years corresponding to a period when sea level fell by 1.5 m, and when about half of the present barrier volume was accumulated. Higher progradation rates are ascribed to the arrival of sediment yielded by an active littoral drift system, which appears to have eroded large extents of several Holocene barriers along 100 km of coastline.

Keywords: Holocene; Barrier; Sea level; Stratigraphy

1. Introduction

Coastal progradation and the establishment of regressive sedimentary sequences occur when the shoreline translates seaward under a condition of excess sediment supply relative to the accommodation space on the shelf (Helland-Hansen and Martinsen, 1996). The translation can occur with stable or slowly rising sea levels (“normal” regression) or be strictly due to a sea level fall (“forced” regression) (Posamentier et al., 1992). In both cases, given wave dominance on coastal processes, a prograded coastal sand body is formed.

Prograded coasts in wave dominated settings are commonly characterized by a series of beach and foredune ridges aligned with the shoreline (strandplain). Progradation associated with slowly rising or stationary sea levels occurs mainly due to a positive longshore sediment imbalance. Examples include the

* Corresponding author. UFBA, Curso de Pos-Graduacao em Geologia, R. Caetano Moura 123, BA 40210-340, Salvador, Brazil. Tel.: + 55-71-237-0408; fax: + 55-71-247-3004.
E-mail address: glessa@pppg.ufba.br (G.C. Lessa).

0025-3227/00/$ - see front matter
PII: S0025-3227(99)00130-9

Galveston Island barrier, in the USA (Davies et al., 1971; Kraft and Chrzastowski, 1985), the Tuncurry barrier, in SE Australia (Cowell et al., 1995; Roy et al., 1995) and the Nayarit beach-ridge plain, in Mexico (Curray et al., 1969).

When progradation takes place under quasi-stable or falling sea level conditions, the coast can also be fed by the erosion of the offshore sea bed, as sand is brought from lower-shoreface and inner-shelf areas (see Swift, 1976). The coastal plain of Caravelas (Domingues et al., 1992), in eastern Brazil, is illustrative. Larger coastal deposits of this kind are reported in areas close to sizeable river mouths, which impose a hydraulic barrier to the longshore sediment transport and cause a strongly positive longshore sediment imbalance. Examples include the Doce, Paraiba do Sul, Jequitinhonha and São Francisco river mouths in eastern Brazil (Dominguez and Wanless, 1991; Domingues et al., 1992).

Depositional sequences associated with "normally" prograded (surplus of sediment under a stationary or slowly rising sea level condition) and "forced" prograded (under falling sea level) are the most likely coastal sedimentary sequences to be preserved in the stratigraphic record, since transgressive sequences are overridden and reworked by the wave ravinement surface and, in a falling sea level scenario, subsequently excavated by a wave diastem, or a regressive surface of erosion (Kraft et al., 1981; Kraft and Chrzastowski, 1985; Roy et al., 1995). There are, however, still few examples in the literature reporting the facies architecture of either normally or forced prograded wave-dominated coastal deposits. The documented stratigraphic investigations on the recent barrier-strandplain deposits developed under a falling sea level appears to be restricted to those of Dominguez and Wanless (1991), on the facies architecture of the Doce river strandplain (Brazil), by Gagan et al. (1994) on the morphostratigraphy of Holocene barrier sequences in northeastern Australia, and by Masselink and Lessa (1995), on the morphostratigraphy of a macrotidal barrier in central Queensland (Australia).

The Paranaguá coastal plain, located in southeastern Brazil (Fig. 1), holds another example of barrier progradation under a condition of slowly falling sea level. Although this coastal plain has had its surface geology extensively unveiled during the last 50 years (Bigarella, 1946; Bigarella, 1965; Riverau et al., 1969; Bigarella et al., 1978; Martin et al., 1988; Angulo, 1992), very limited attention has been given to the nature of the underlying sedimentary strata (Maack, 1949; Bigarella et al., 1978), and only a rough attempt has been made to define the three-dimensional geometry of the surface deposits (Lessa and Angulo, 1995). This study aims to provide a more detailed stratigraphic documentation on this coastal plain, and to propose a framework for the evolution of this coastal setting in the mid- to late-Holocene.

2. Study area

The Paranaguá-Laranjeiras estuarine system defines two main prograded barriers in the coast of Paraná State: the Paranaguá barrier in the south and Superagui-Peças barrier islands in the north (Fig. 1). In both barriers, beach/foredune ridges with orientations similar to the present coastline, are the prevailing surface deposits. The ridges are subdivided between late Pleistocene (ca. 120 000 years B.P.) and Holocene (younger than 5100 years B.P.) ages, based on morphological, elevational and radiocarbon evidence (Martin et al., 1988; Angulo, 1992; Angulo and Suguio, 1995).

Pleistocene and Holocene deposits in the Paranaguá coastal plain are separated by a topographical depression associated with the Guaraguaçu River (Figs. 1a and 2), which attains an average of +2 m above mean sea level (MSL). This depression is interpreted as a paleo-lagoonal zone associated with the last (5100 years B.P.) sea level maximum (Martin et al., 1988; Angulo, 1992; Lessa and Angulo, 1995). The general barrier surface dips seaward both in the Pleistocene and Holocene sectors, indicating progradation under a falling sea level. Maximum and minimum elevations, observed in the west and east side, respectively, are about +11 and +4 m in the Pleistocene and +5.3 and +2.2 m (present back-shore) in the Holocene barrier. Barrier topography likely reflects the elevation of relict backshores, as few dunes, especially by the coastline, are recognized on the plains (Angulo, 1992). Thermo-luminescent datings of the Pleistocene barrier provided ages varying from 105.510 to 85.785 years B.P. (Barreto et al. 1999), whereas ^{14}C datings of shells, tree trunks and vegetal debris within the Holocene barrier provided ages

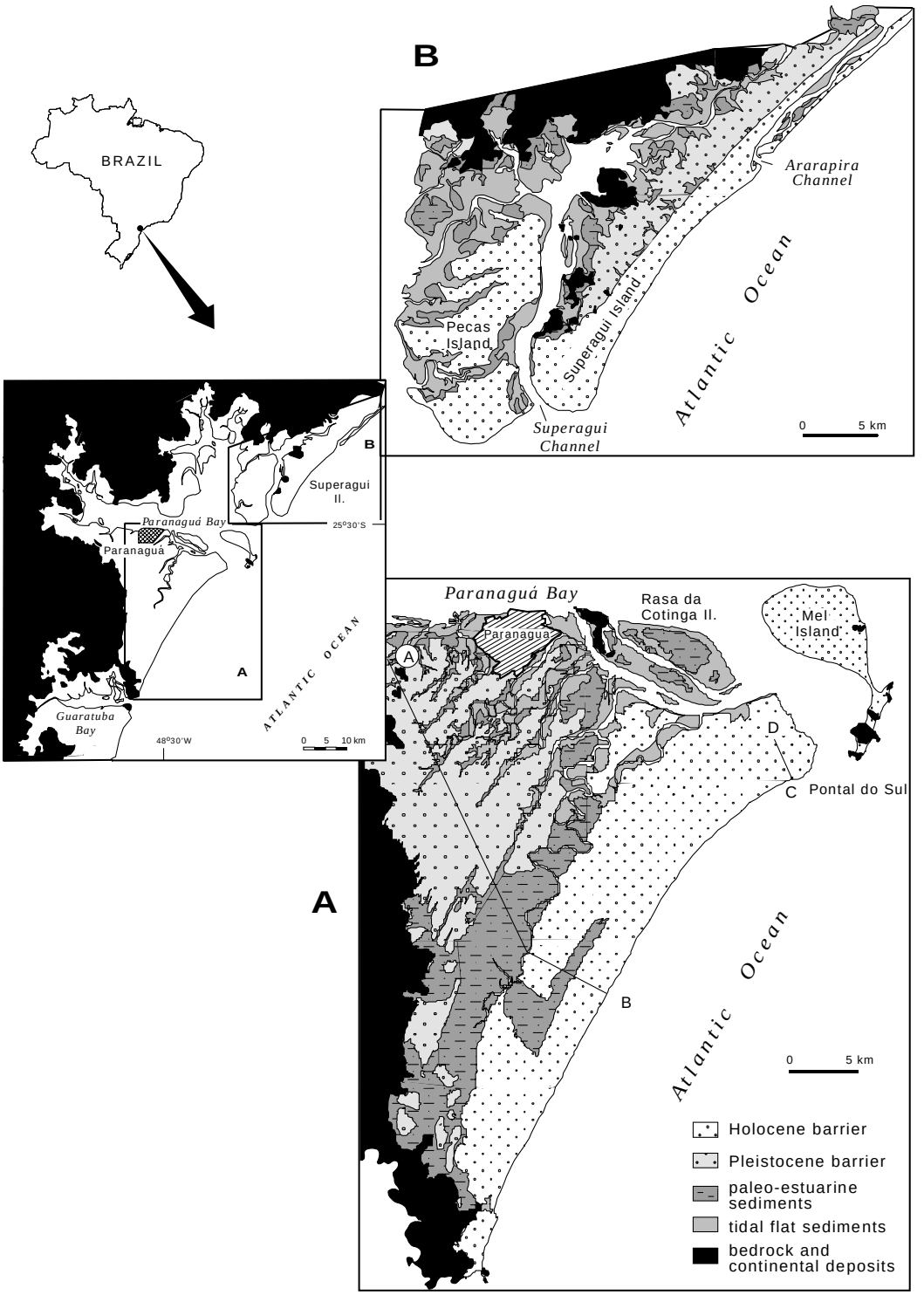

Fig. 1. The coastal plain in the State of Paraná, and the surface geology of the Paranaguá (inset A) and Superagui and Peças Island (inset B) coastal plains.

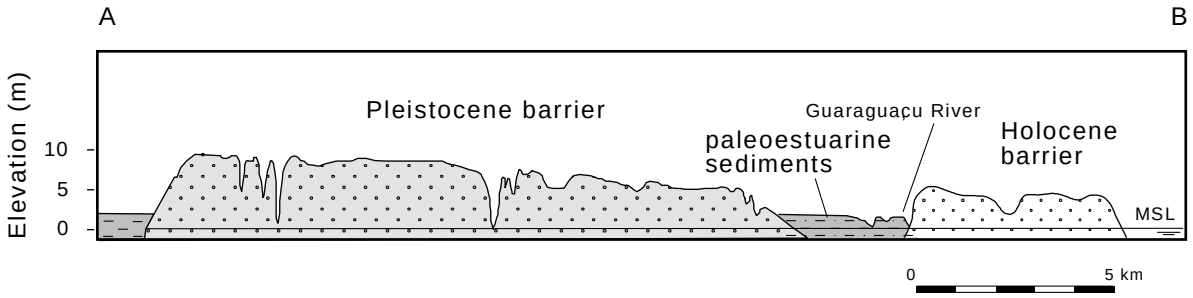

Fig. 2. Topographical profile normal to the Paranaguá coastal plain (after Bigarella et al. 1978—see Fig. 1a for location), and basic geological framework for the Quaternary sedimentary deposits as mapped at the surface (after Angulo, 1992).

varying from 6.520 to 3.960 years B.P. (Angulo et al. 1999).

In the Superagui coastal plain (Fig. 1b) the inter-barrier depression is non-existent, and the Holocene marine deposits direct onlap the Pleistocene. The head of several paleo-streams incised in the Pleistocene barrier are cut off, suggesting that the Holocene barrier overstepped the Pleistocene barrier during the final phases of the post-glacial marine transgression (PMT). Very few data exist for the Pleistocene barriers in Paranaguá and Superagui, and a hypothesis that they may in fact contain more than one generation of Pleistocene barrier cannot be overruled.

The spring tide range is 1.8 m at the mouth of the Paranaguá bay estuary, but decreases slightly both south- and northwards along the coastline (Harari and de Camargo, 1994). The coast is classified as an open coast, exposed either to the E–NE or SE–S waves. Reliable wave statistics are restricted to a couple of short term measurements campaigns, the longest comprising the deployment of a wave-rider buoy 13 km offshore ($\cong$ 20 m water depth) between August and December 1982 (PORTOBRAS, 1983). The results (Table 1) show that wave approach is mainly from ESE to SE, with a mean significant wave height of 1.8 m and a mean wave period of 11 s.

Several lines of morphological evidence indicate a northbound littoral drift. In plan view, the orientation of the beach ridges suggest a south-to-north direction of progradation: the ebb tidal deltas are more pronounced in the southern side, and river outlets are steered to the north (Angulo, 1995b). Sayão et al. (1989) estimated that about 0.3×10^6 m^3/year of sand moves northward close to the Paranaguá bay mouth. This net drift is observed through off-sets of estuary entrances along the coast (Tessler, 1988) and significant sand accumulation at the southern side of ebb-tidal deltas. Based on the reports of regular dredging operations executed by the harbor authority at the bay mouth, a total of 7.8×10^6 m^3 of sand has been taken from the navigation channel between 1987 and 1993, with a yearly average of 1.1×10^6 m^3 (APPA, 1994). The majority of this volume came from the channel dredged across the ebb-tidal delta, that now acts like a trap, and thus gives an approximate rate of longshore transport in that area. The trapped volume of sand seems to be at least twice as large as calculated through empirical formulas (Sayão et al., 1989). Soares et al. (1994) report a coastal progradation amounting to 559 000 m^3 in 50 years in Pontal do Sul, at the southern side of the bay mouth. The progradation might have been caused by the construction of

Table 1
Monthly characteristics of the waves offshore of the study area between 21/08/1982 and 21/01/1983 (intermittent measurements)

	August	September	October	November	December
Maximum height (m)	2.35	3.95	3.20	2.65	3.50
Significant height—Hs (m)	1.58	2.54	2.04	1.49	2.13
Mean period (s)	16.53	10.73	12.00	9.80	12.00
Direction (°)	–	112	133	140	123

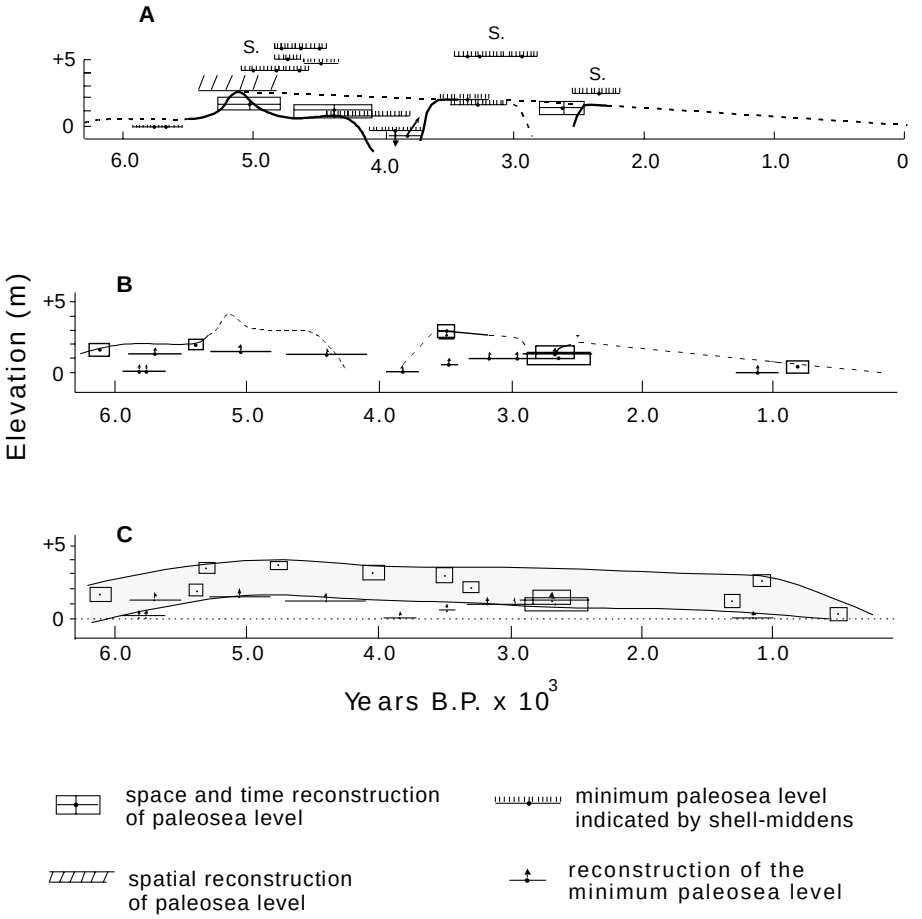

Fig. 3. Proposed sea level curves for the study area: (a) Suguio et al. (1985); (b) Angulo and Suguio (1995); and (c) a sea level envelope (after Angulo and Lessa, 1997). Elevations are in relation do mean-sea level.

a jetty inside the main channel, and therefore might be associated with a longshore sediment transport towards the estuary. This gives a transport rate of 11 200 m^3/years, which is much lower than those above. Such lower rates could be explained by the fact that the prograded area is inside the domain of an ebb tidal delta, and that the volume of sediment involved in the progradation is underestimated since sedimentation below MSL was not considered.

2.1. Late Holocene sea level trend

The first sea level curve proposed for the study area (Fig. 3a) (Suguio et al., 1985) followed the same general contour of the other seven regional sea level curves that have been proposed for different sites on the Brazilian coast (Suguio et al., 1985). A general fall of sea level would have occurred after a maximum of about +2.5 m at around 5100 years B.P., interrupted by two intervals of pronounced negative oscillations when sea level would have been at, or below, the present elevation (4100–3800 and 3000–2700 years B.P.). With new ^{14}C datings for the coastal plain and re-evaluation of some archaeological data, Angulo and Suguio (1995) showed that the transgression maximum was higher than previously suggested (Fig. 3b). More recently, a re-evaluation of the paleo-sea level data utilized to define the first curve and a new set of vermetid worm tube datings allowed Angulo and Lessa (1997) to propose that the Holocene

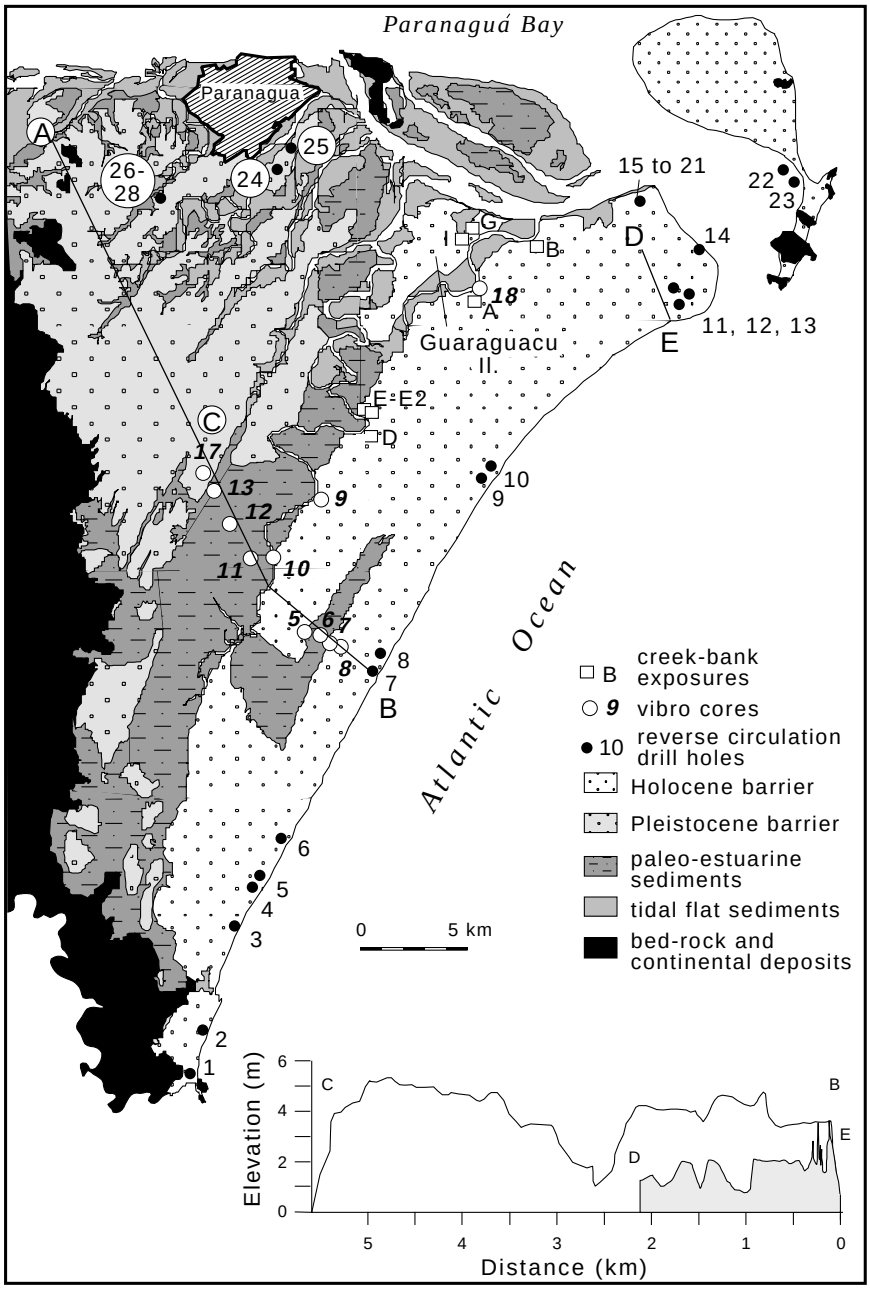

Fig. 4. The surface geology of Paranaguá coastal plain (after Angulo, 1992), with the location of the reverse circulation cores, vibro-cores, creek-bank exposures and the line traversed by the stratigraphic profiles (Fig. 9). The inset shows the elevation difference of two topographical profiles on the Holocene barrier.

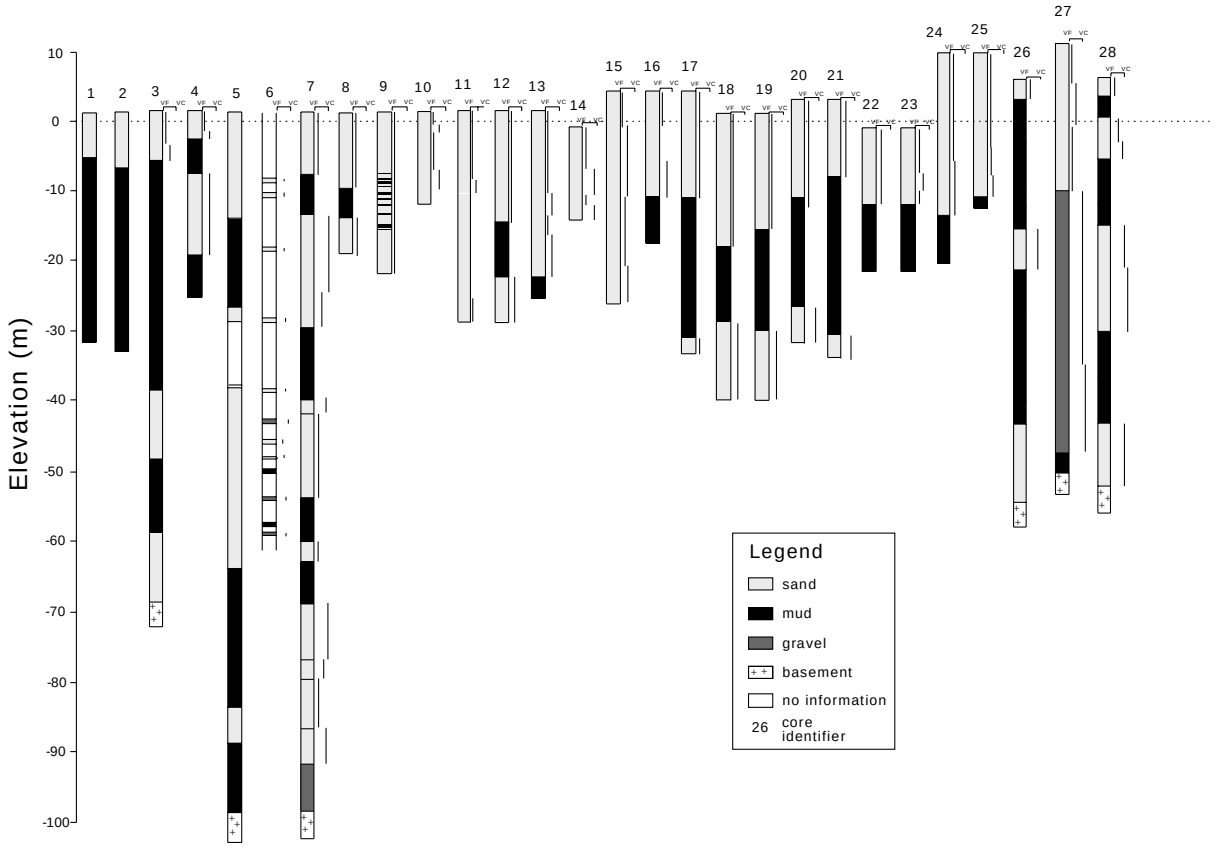

Fig. 5. General interpretation of the reverse circulation cores. Elevation in relation to mean sea level.

sea level maximum was about +3.5 m. Moreover, the evidence for higher frequency, large amplitude sea level oscillations in the late Holocene are disputable (see also Lessa and Angulo, 1998). Therefore, a smoother decline of sea level since the end of the PMT appears to characterize the sea level trend (Fig. 3c).

3. Data sources

Fig. 4 shows the location of 28 reverse-circulation drill holes (Rc) on the coastal plain. Rc#7 was published by Maack (1949), and Rc#4, #5, #6, #10, #16 and #24 were published by Bigarella et al. (1978). The remaining cores derived from the geotechnical work performed by engineering companies in the area. Rc#1 to #21 came from the Holocene barrier, Rc#22 and #23 from an eroded barrier platform (about 1 m below MSL) in Mel Island and Rc#24 to #28 from the Pleistocene barrier. Fig. 5 presents the lithology of all drill holes, based on the driller's technical logs. It must be emphasized that these logs were written at different times by different technicians, so that consistency is jeopardized. Besides, their aim was to differ the bulk qualities of the sub-surface deposits, and accuracy becomes limited. Therefore, attention is only given to the most general characteristics of the sedimentary deposits.

Ten cores from the Holocene and one from the Pleistocene sector of the coastal plain were taken with a vibro-corer, utilising 6 m long, 0.75 mm wide aluminum barrels. Their locations are shown in Fig. 4. Vibro-cores #5–#17 were aligned normal to the

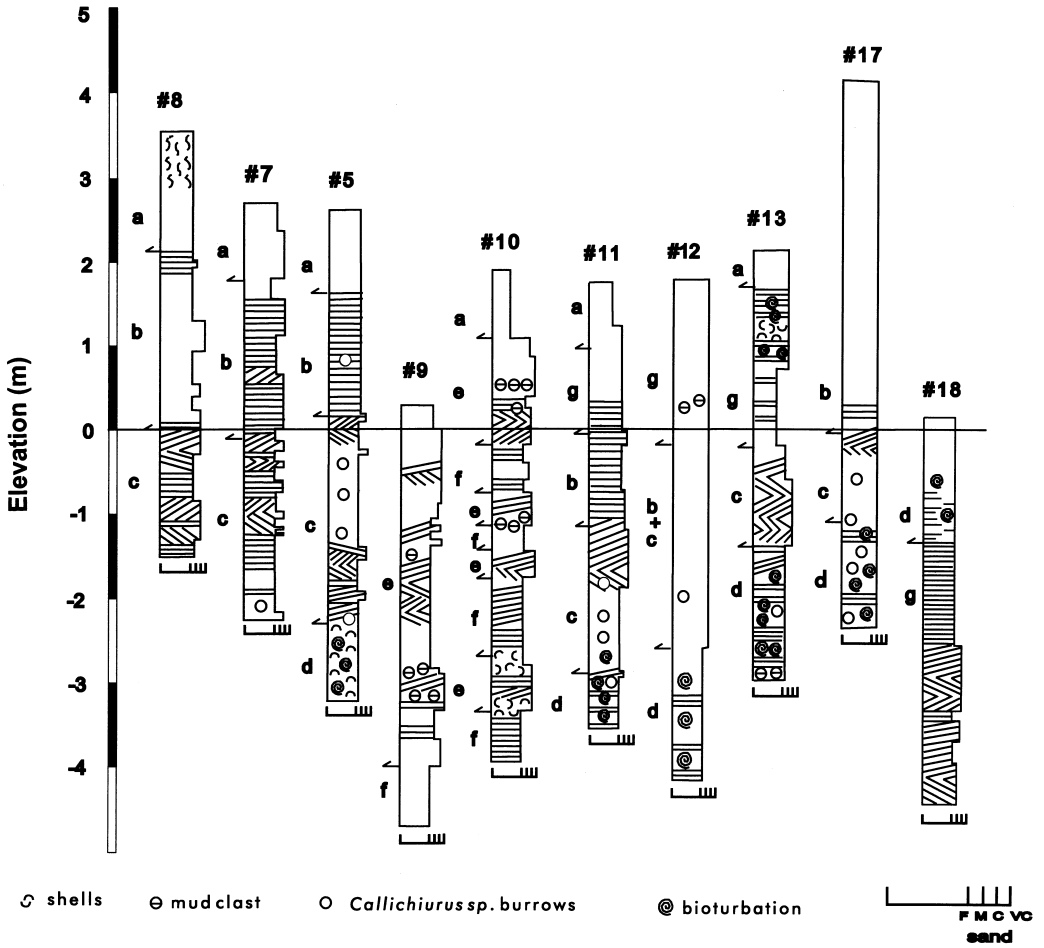

Fig. 6. Grain size variation, sedimentary structures and interpreted sedimentary facies (between arrows at the left side of each column) along the vibro-cores (see location in Fig. 4). a = undifferentiated; b = beach face; c = nearshore; d = upper-shore face; e = estuary channel; f = overwash; g = tidal flat; h = flood-tidal delta (codes also applied to Fig. 7). Sedimentary structures are always plane-parallel, horizontal or inclined.

coastline in the center of the coastal plain, between the shoreline and the outer limit of the Pleistocene barrier. Vibro-cores #5–#8 were taken from the vicinity of a topographic depression probably related to a paleo-tidal inlet (see also Fig. 2). Vibro-core #9 was taken at the very base of a scarp at the rear of the Holocene barrier and vibro-cores #10 to #13 were collected on the Guaraguaçu river plain. Vibro-core #18 was taken from the base of another logged channel bank exposure at the rear of the Holocene barrier. All these cores were leveled in relation to established bench-marks, with the exception of vibro-cores #9 and #18, where elevation was assessed relative to the local high-tide mark (datum given by the tide gauge in Paranaguá harbor—see Fig. 1). Due to difficulties in extruding, vibro-core #6 had to be vibrated out, which caused the loss of the sedimentary structures.

In the laboratory the cores were split length-wise, photographed and logged (Fig. 6). Grain size was visually estimated. Sixty-two samples taken from different sections of vibro-cores #7, #8, #10, #11, #12 and #17 (Holocene barrier, inter-barrier depression and Pleistocene barrier) had their heavy mineral assemblages determined. The very fine sand fraction

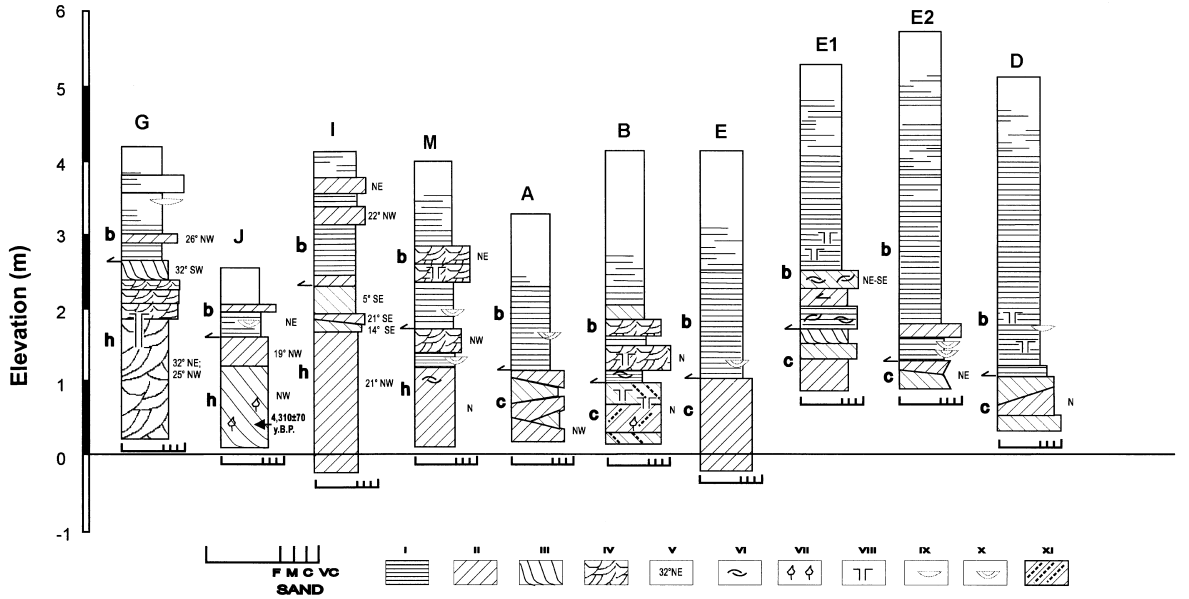

Fig. 7. Grain size variation, sedimentary structures and interpreted sedimentary facies (letters at the left side of each column) along the creek-bank exposures (see location inFig. 4). Codes for the sedimentary facies are given in Fig. 6. I = plane-parallel stratification; II = tabular cross-stratification; III = tabular cross-stratification tangent at the base; IV = trough cross-stratificiation; V = strike and dipping angle; VI = shells; VII = organic detritus; VIII = *Callichirus sp*. burrows; IX = coarser sediment lens; X = small channel fill; XI = mud laminae in the forests.

(3–4ϕ) of each sample was chosen for densimetric separation with bromoform ($CHBr_3$). This fraction is the hydraulic equivalent of the modal class (fine sand in all samples), and contains the mode of the heavy minerals size distribution. The transparent, non-micaceous heavy minerals were quantified to at least 100 grains, utilizing the "ribbon method" (Galehouse 1971). The minerals were separated in ultra-stable (zircon, turmaline and rutile), meta-stable (staurolite, apatite, epidote, kyanite, sillimanite, garnet) and unstable (hornblende, hypersthene, augite, andaluzite) minerals, and their relative abundance in each sample calculated.

Additional information on the upper sedimentary sequence of the Holocene barrier, as well as on the direction of paleo-flows (following the measurement of the primary sedimentary structures), were gathered at several other bank exposures along the erosive margins of tidal channels at the rear of the Holocene barrier (Fig. 4). The true elevation of these outcrops was also estimated by the high-tide mark. The interpreted sections are shown in Fig. 7.

4. Results

4.1. Reverse circulation cores

The lithologic interpretation of the Rc drill holes by Maack (1949) suggested that the upper 70 m of sediments beneath the coastal plain (Rc#7) are Holocene marine deposits, which overlie 31 m of Pleistocene marine sedimentation (Fig. 5). Bigarella et al. (1978) interpreted the sand layers of the Rc#10, #11, #12 and #24 as transgressive and regressive marine sequences, and Rc#3 and #4 as a regressive marine sequence. Invariably, underlying the top sandy unit, there is a deposit represented by a dark-colored, organic- and mud-rich sediment, interpreted by Bigarella et al. (1978) as paleo-lagoonal. In Rc#4 and #7 (Fig. 5), the top mud unit was interpreted by Bigarella et al. (1978) and Maack (1949), respectively, as transgressive marine. Only a few samples were taken from Rc#6, and Bigarella et al. (1978) have suggested that only the top 25 m corresponds to marine deposition. Overall, Bigarella

et al. (1978) did not differentiate chronological boundaries in their interpretation.

With the exception of Rc#6 (which is fragmented), and Rc#11, #14 and #15 (that come from the northern end of the Holocene barrier), all drill holes present a superficial layer of fine sand, with thickness varying from 8 to 21 m, overlying dark-colored, organic- and mud-rich sediments. An exception is Rc#5, where beneath the top layer of sand there is a layer of white, plastic mud. A second layer of fine-to-coarse sand appears in Rc#4, #7, #8, #12 and #17 to #21. Overall, it is observed that there are two recurrent sedimentary units amongst the profiles: a yellowish upper sand layer and an organic- and mud-rich dark unit underneath. The top unit is interpreted here as Holocene barrier sand, based on the nature of the surface sedimentation (marine) in the whole coastal plain (more than 25 km wide) and due to the fact that a Holocene/Pleistocene boundary within marine deposits has been identified inland from the drilling sites (Angulo 1992; Angulo and Suguio 1995). The underlying mud layer is interpreted here as a Holocene transgressive estuarine/lagoonal deposit, based on the assumption that the inter-barrier estuarine environment presently observed was a persistent feature behind a rolling barrier adapting to the post-glacial sea level rise. It is difficult to define a sedimentation pattern below this mud layer, although another sand unit is often observed as a third layer. In Rc#24–#28 the sand and organic muddy units can also be interpreted as barrier and transgressive estuarine deposits, but of the Pleistocene age.

The basement was reached in Rc#3, #5, #7, #26, #27 and #28 (Fig. 5). Minimum (farther inland) and maximum (close to the shoreline) depths are about −50 and −100 m, respectively. Talus, alluvial fans and debris flow deposits, varying in age from Miocene to Quaternary (Lima and e Angulo, 1990; Angulo, 1995a), have been mapped on the surface between the rear of the marine deposits and the coastal mountain range. Therefore, it is expected that Cenozoic continental/alluvial sediments exist between the marine sedimentation and the bedrock underneath, especially in the landward reaches of the coastal plain. The logs for Rc-cores #26, #27 and #28 actually mention the existence of feldspar as well as poorly sorted, very coarse sand at a certain point along the cores, which is rather different from the more mature, finer and better sorted sands of the Pleistocene and Holocene barriers.

4.2. Vibro-cores and creek-bank exposures

Figs. 6 and 7 show the grain size variation and sedimentary structures observed in the vibro-cores and exposures along the creek margins. Sediments are mainly quartzose sand. Observed sedimentary structures varied amongst plane-parallel laminations, cross laminations, large scale sets of cross stratification (in the exposures) and bioturbation (including tubes and burrows of *Callichirus* sp.). On the basis of the sedimentary structures and bounding surfaces, textural and mineralogical composition, color and distance from the shoreline, seven sedimentary facies were distinguished.

(1) *Beachface (facies b):* is comprised of well-sorted very fine to medium sand, brown, light brown and light gray in color. Sedimentary structures consist mostly of plane-parallel, thin to medium laminae (not thicker than 2 cm) (Fig. 8a). Occasionally, a thin to medium set (no thicker than 30 cm) of inclined plane-parallel laminae (as in vibro-core #7 and exposures G, I, M, A, E and E2) is observed, which is ascribed to the fills of shallow longshore channels that occur on the beach face behind swash bars. Bioturbation, which becomes more frequent with depth, is restricted to the presence of burrows and tubes (Ophiomorpha) attributed to *Callichirus sp*., a crustacean that preferably lives between MSL and low tide level (Suguio and Martin, 1976). Disturbed laminae, related to the collapsing of narrow sections overlying the burrows, are also observed. This facies was observed in all of the vibro-cores and exposures, with the exception of vibro-cores #9 and #10, which are marginal to the river. Maximum and minimum elevations of this facies were +5.0 m (exposure E in the back-barrier) and −1.2 m (vibro-core #11, in the middle of the inter-barrier depression), respectively.

(2) *Nearshore (facies c):* is comprised of well-sorted fine to coarse sand, mostly gray and light gray in color (Fig. 8a). The facies was identified both in the vibro-cores (#5, #7, #8, #11, #12, #13, #17 and #18), and in the exposures (E, E1, E2, D, A and B). Cross-stratification (planar and trough) is the prevalent sedimentary structure in the exposures, dipping between 13 and 29° towards NE and SE

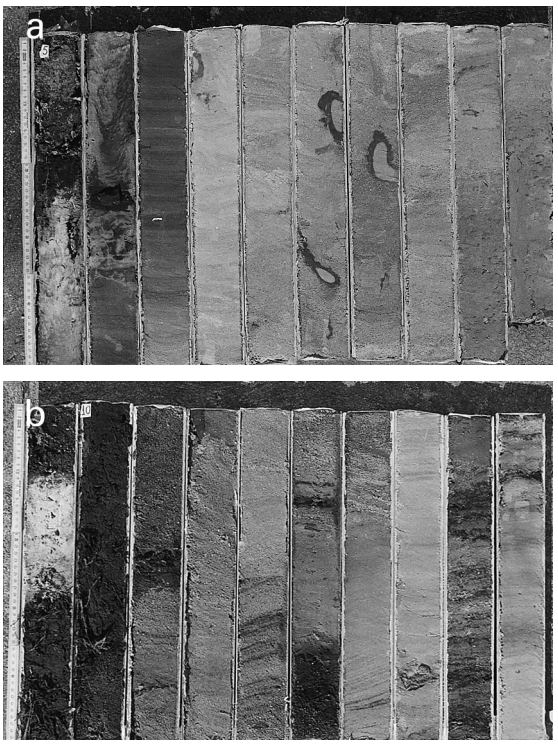

Fig. 8. (a) Photograph of core #5, taken in the middle of the Holocene barrier (see Fig. 4), showing a regressive barrier sequence with beach, nearshore and upper shoreface sediments (see Fig. 6 for interpretation). The tubes are 0.5 m long (metric scale at left), and depth increases from left to right. Stained (darker) sandy sediments between 0.5 and 1.5 m is due to the development of a podzol soil and rounded, darker scars between 1.5 and 3.5 m are ascribed to *Callichiurus* sp. tubes. (b) Photograph of core #10, taken from the floodplain at the rear of the Holocene barrier, showing the interfingering of estuarine (highly stained, coarser, poorly sorted channel sediment) and overwash (finer, light gray and well-sorted sand) deposits. The tubes are 0.5 m long (metric scale at left), and depth increases from left to right.

(alongshore) and forming sets up to 1.5 m thick (exposure E). In the vibro-cores the unit shows inclined sets of plane-parallel laminations dipping in opposite directions. Burrows and tubes (Ophiomorpha) also attributed to *Callichirus* sp. abound (Fig. 8a), and molds of bivalve shells (dissolved by humic acids) are also noticed. Maximum and minimum elevation of this facies was +0.1 m (vibro-core #5, in the middle of the barrier) and −3.0 m (vibro-core #11, in the middle of the inter-barrier depression), respectively.

(3) *Upper shoreface (facies d):* is comprised of well-sorted fine to very fine gray to light gray sand. Very thin to thin (less than 1 cm thick) mud laminae are occasionally found. Bioturbation is the most typical sedimentary structure of this facies, which also harbors molds of bivalve shells, burrows (of *Callichirus* sp.) and eventually horizontal sets of plane-parallel laminations (associated with mud laminae) (Fig. 8a). This facies was only observed in the vibro-cores, as its upper boundary is below low water level. Maximum logged elevation was −1.2 m (in vibro-core #17, the innermost position in the cross-section profile—Fig. 4) and minimum elevation is unknown since no core completely crossed the unit.

(4) *Estuarine channel (facies e):* this unit was restricted to vibro-cores #9, #10 and #18 (at the rear edge of the barrier). In cores #9 and #10 it is comprised of poorly sorted, fine to very coarse sand, showing varying degrees of reworking of the sand grains (from rounded to angular) (Fig. 8b). The color varies from light gray to gray and brown to dark-brown. Very thin to thin, texturally different laminae are inclined (10° to 30° dip), and are normally associated with mud clasts. Layers of bivalve shell molds and shell fragments were observed in vibro-cores #10 and #13.

This facies in vibro-core #18 is characterized by better sorted marine sands, with a general fining upward trend. The upper meter of this core shows signs of ripple cross-stratification probably associated with shoaling waves, which would precede the formation of a nearshore zone as identified in exposure A (Fig. 7). Below this level, a tidal channel signature is suggested by a cyclic change in the thickness (bundles?) of sub-horizontal laminae in the upper meter of this unit. Dip angles varying between 20 and 30° toward the continent characterizes the lower 2 m of the unit.

Maximum and minimum elevation of this facies were +1.6 m (vibro-core #13) and −7.7 m (vibro-core #18).

(5) *Overwash (facies f):* comprised of well-sorted, very fine to medium light gray and light brown sand. The unit is restricted to vibro-cores #9 and #10 (at the rear edge of the barrier—Fig. 8b). Sedimentary structures are sub-horizontal sets (5–10° dip towards the continent) of plane-parallel lamination. Maximum and minimum elevation of this facies were −0.1 and −3.9 m, respectively, both in vibro-core #10.

(6) *Tidal flat (facies g):* comprised of laminations of fine sand and mud, mostly bioturbated. The unit is restricted to vibro-cores #11, #12 and #13, in the inter-barrier depression. It is more extensive in vibro-core #13, where it attains 2.3 m in thickness, and fines downwards. The lowest section in this core is very clayey with some lenses of medium sand. Maximum and minimum elevation of this facies were +1.7 m (in vibro-core #12) and −0.2 m (in vibro-core #13), respectively.

(7) *Flood-tidal delta (facies h):* Mostly tabular cross-stratified sets varying in thickness between 0.5 and 1.5 m, dipping 5–30° predominantly to NW (towards the estuary). Alternating laminae of fine, medium and coarse sand, which coarsen gradually towards the base, characterize the structures. Laminae of mud and organic detritus are also observed between the sand laminae, especially closer to the base. A piece of a tree, collected at the base of exposure J (Fig. 7) was dated at 4310 ± 70 years B.P. ($\delta^{13}C = -29.7$) (CENA 120).

5. Interpretation and discussion

5.1. Shorenormal morphostratigraphy

Fig. 9a shows a cross-section normal to the shoreline along the middle of the coastal plain. The basement depth below the Pleistocene barrier was based on Rc#26, and the thickness of the sedimentary facies, schematically drawn, based on Rc#24–#28 (see Fig. 5). It is observed that two generations of regressive barriers are identified. The Pleistocene barrier seems to be much larger than the Holocene, both in respect to depth and width, and it is even possible that more than one generation of Pleistocene barrier deposits exists. In fact, three generations of Pleistocene barrier systems are reported in the southernmost coastal plains in Brazil (State of Rio Grande do Sul—Villwock et al., 1986). The thickness of the Pleistocene barrier in Rc#24–#28 varies from 2 m to over 20 m, which is more than twice the thickness of the Holocene barrier in Rc#7.

A detailed cross-section of the stratigraphy of the Holocene barrier is shown in Fig. 9b. The figure shows the Pleistocene barrier forming the substrate for the Holocene sedimentation. Paleo-estuarine sediments underlie the Holocene barrier, which is subdivided into transgressive and regressive deposits. The former is distinguished by the existence of marine sands (overwash deposits) intercalated with tidal-channel sands (in vibro-cores #9 and #10) and the surface morphology (a smooth landward dipping profile fronted by a beach ridge). The Pleistocene age for the sand deposit beneath the inter-barrier depression is suggested by the elevation of the sedimentary facies and low relative quantities of unstable heavy minerals. An analysis of the samples taken from the inter-barrier depression (vibra-cores #11, #12 and #17) and Holocene barrier (vibro-cores #7, #8) show that unstable minerals account for an average of 13% of the heavy mineral content in the inter-barrier depression whereas they account for an average of 43% in the Holocene barrier. This contrast indicates that the marine deposits observed in vibro-cores #11, #12, #13 and #17 are much older than those in the Holocene barrier, i.e., they have undergone a longer period of mineral dissolution. Differences in the unstable heavy mineral relative amounts between Holocene and Pleistocene barriers have been reported in other coastal plains in south Brazil (Mio and Giannini, 1997).

Barrier progradation concomitant with a sea level fall is indicated by the elevation difference between the beach and nearshore facies contact in three sections of the Holocene barrier (Fig. 9b). An average elevation of +1.4 m at exposures D, E1 and E2, at the rear of the barrier, falls to approximately 0.5 m in vibro-cores #5, #7 and #8 in the middle of the barrier, and finally to about −0.5 m at the coast (Araújo and Lessa, 1996). Based on the sedimentary structures only, a sea level fall of approximately 2.9 m would have occurred in the time span of barrier progradation, a value which is close to 3.5 m proposed by Angulo and Lessa (1997) based on several radiocarbon datings of paleo-sea level indicators.

This same contact elevation between beach and nearshore facies in the exposures A, B, E, E1, E2 and D (Fig. 7) is about 2.5 m higher than that observed in the Pleistocene barrier (vibro-cores #11 and #12, Fig. 6). The elevation difference in the facies contact could imply one of the following: (i) that sea level associated with the seaward end of the Pleistocene barrier at 120 000 years B.P was lower than the Holocene sea level maximum, which would be in

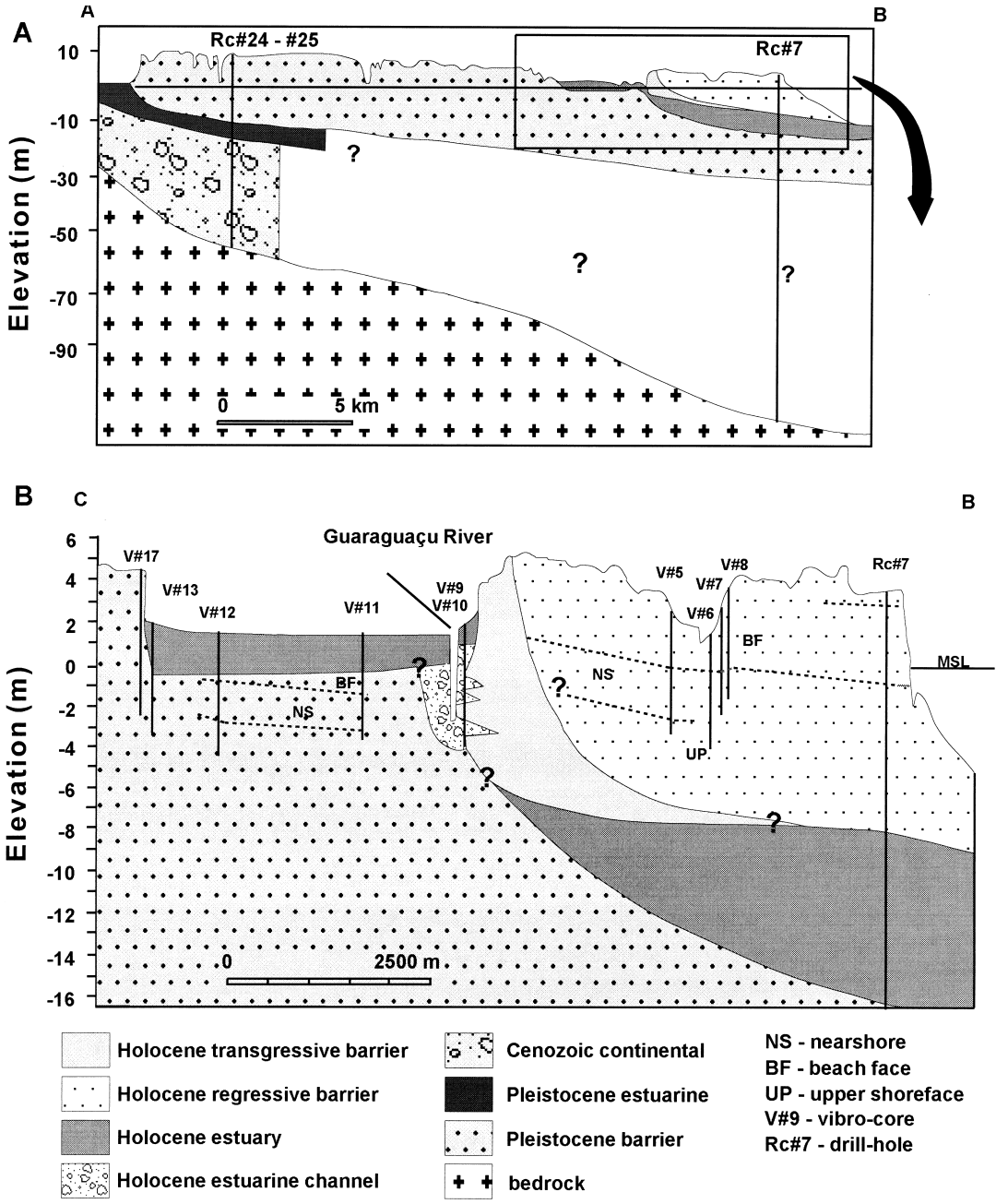

Fig. 9. (a) general stratigraphic cross-section normal to Paranaguá coastal plain; (b) detailed stratigraphic cross-section normal to the Holocene barrier (see Fig. 4 for location). Lines separating the sedimentary facies were traced based on elevations indicated in Figs. 6 and 7. The contact between the beach and nearshore facies at the coastline is about −0.6 m (Araújo and Lessa, 1996).

accordance with the difference in the surface elevation between the barriers (Fig. 2); or (ii) that the Pleistocene barrier deposit under the inter-barrier depression is a remnant of a younger Pleistocene barrier, with an age of approximately 85 000 years B.P. (isotope stage 5c, see Roy et al., 1995), and associated with a sea level maximum lower than the present one, which is yet to be identified in the Brazilian coast.

The presence of paleo-estuarine/lagoonal deposits underneath the barrier indicates that the barrier has transgressed over an estuarine environment as the sea level rose. The first stratigraphic model of the coastal plain (Lessa and Angulo, 1995), based on the drill-holes only, suggested that the organic-mud deposits beneath the barrier were a sub-surface extension of the paleo-estuarine deposits mapped in the inter-barrier depression. Vibro-cores #11–#13 show, however, that the paleo-estuarine deposits in the inter-barrier depression are restricted to the top 2 m of the profile, and that a connection to similar deposits under the Holocene barrier may not exist. The Holocene barrier appears to have encroached onto the Pleistocene barrier (an encroached Holocene barrier is observed in Superagui Island—Fig. 1b). However, owing to the presence of the Guaraguaçu River flowing along the inter-barrier depression, both the Holocene and Pleistocene barriers were eroded as the river was restricted near the end of the Holocene transgression.

The presence of more than 5 m of estuarine mud beneath the present shoreline (Fig. 5) suggests that a much larger estuary was present when sea level was some 10 m below present, and the paleo-coastline was several kilometers offshore. As sea level rose, the estuary shrunk, possibly due to a steepening of the substrate slope. More energetic, confined flows would have given rise to the coarse estuarine sand deposits observed in vibro-cores #9 and #10, and may also have been responsible for the erosion in the contact between the barriers. While erosion of the Pleistocene barrier is well indicated by the sharp contact between the estuarine and beach deposits in vibro-cores #11–#13 (Fig. 6), evidence of a wider Holocene barrier is found in the exposures along the estuarine channel (exposures E, E1, E2 and D). Sedimentary structures observed in the northern half of the barrier are not related to a transgressive deposit, such as landward inclined, parallel or wavy laminated sets and convolute laminae (Murakoshi and Masuda, 1992). Instead, cross-stratification associated with longshore flows in the nearshore abound (Fig. 7). The erosion of the transgressive barrier by the river appears to be the most convincing explanation for the observation of foreshore and nearshore sedimentary structures at the rear of the Holocene barrier.

Fig. 10 illustrates a sequence of events that lead to the erosional situation mentioned above at the northern half of the inter-barrier depression (with no intention to reproduce the detailed morphostratigraphy). The transgressive barrier was moving over paleo-estuarine sediments (Fig. 10a) as sea level rose. The transgression was still operative in Fig. 10b, but due to a higher substrate gradient the moving barrier starts compressing the estuary against the Pleistocene shoreline. The succession of events in Fig. 10c and d might have been simultaneous. The transgressing barrier encroaches on the Pleistocene barrier and the estuary channel clears its way between them. The seaward side of the Pleistocene barrier, as well as part of, or perhaps the entire, transgressive barrier, is eroded by the estuarine flow. The following sea level fall (Fig. 10d) caused coastal progradation, exposed the erosive margin at the rear of the Holocene barrier and left a drape of estuarine sediments over the scrapped Pleistocene barrier platform.

Vibro-core #6, taken from the inter-barrier depression in the middle of the Holocene barrier (Fig. 4), which has always been mapped as a muddy, inter-barrier paleo-estuarine feature, revealed only sandy deposition. This morphological feature is reinterpreted as a previous outlet of the Guaraguaçu River estuary during the highstand. At this time, with MSL at approximately $+3.5$ m, an estuary tidal prism of about 60×10^6 m^3 could have allowed for the existence of a second inlet, in addition to an exiting point to the north. As sea level fell, the tidal prism was reduced and the tidal currents became less efficient. The channel became shallower, less tidal and its orientation was then changed by the S–N longshore drift, causing its northward orientation. The continuously lowering sea level eventually closed the inlet. This hypothesis is presently under examination.

5.2. Comparative barrier morphostratigraphy and active shoreface profile

Four stratigraphic cross-sections normal to the

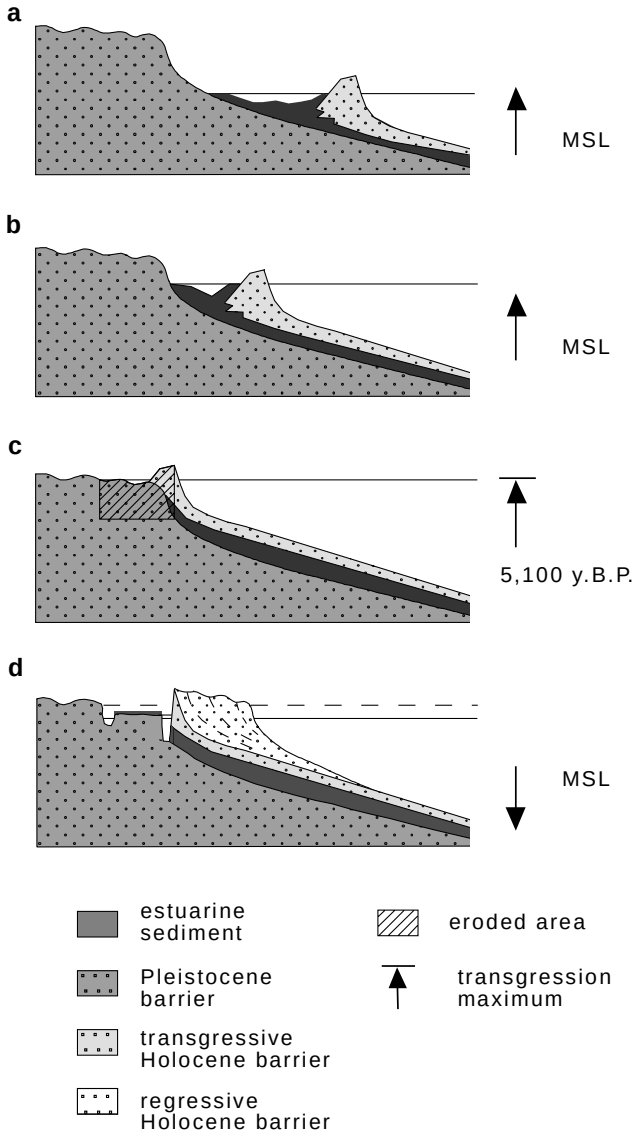

Fig. 10. Schematic evolution of the encroachment process proposed for the Holocene barrier onto the Pleistocene barrier, and the resulting erosion ascribed to the squeezed Guaraguaçu river estuary.

coastline associated with different barriers are shown in Fig. 11: two associated with forced regression (Paranaguá and Bucasia) and two associated with normal regression (Tuncurry and Galveston). The toe of the modern shoreface can be indicated by the contact between the regressive sand facies and the underlying substrate (paleo-estuarine mud, transgressive sands and lower shoreface muds). Shallower shorefaces, terminating before −10 m, are observed in the low energy, wind-wave dominated coasts of NE Australia ($H = 0.75$ m and $T = 6$ s, Masselink and Lessa 1995) and the US Gulf Coast. A deeper shoreface, with depths around −20 m, is indicated in the high energy, swell dominated coast of SE Australia ($H = 1.5$ m and $T = 10$ s, Short 1984). The coast of Paranaguá can be classified as a moderate energy

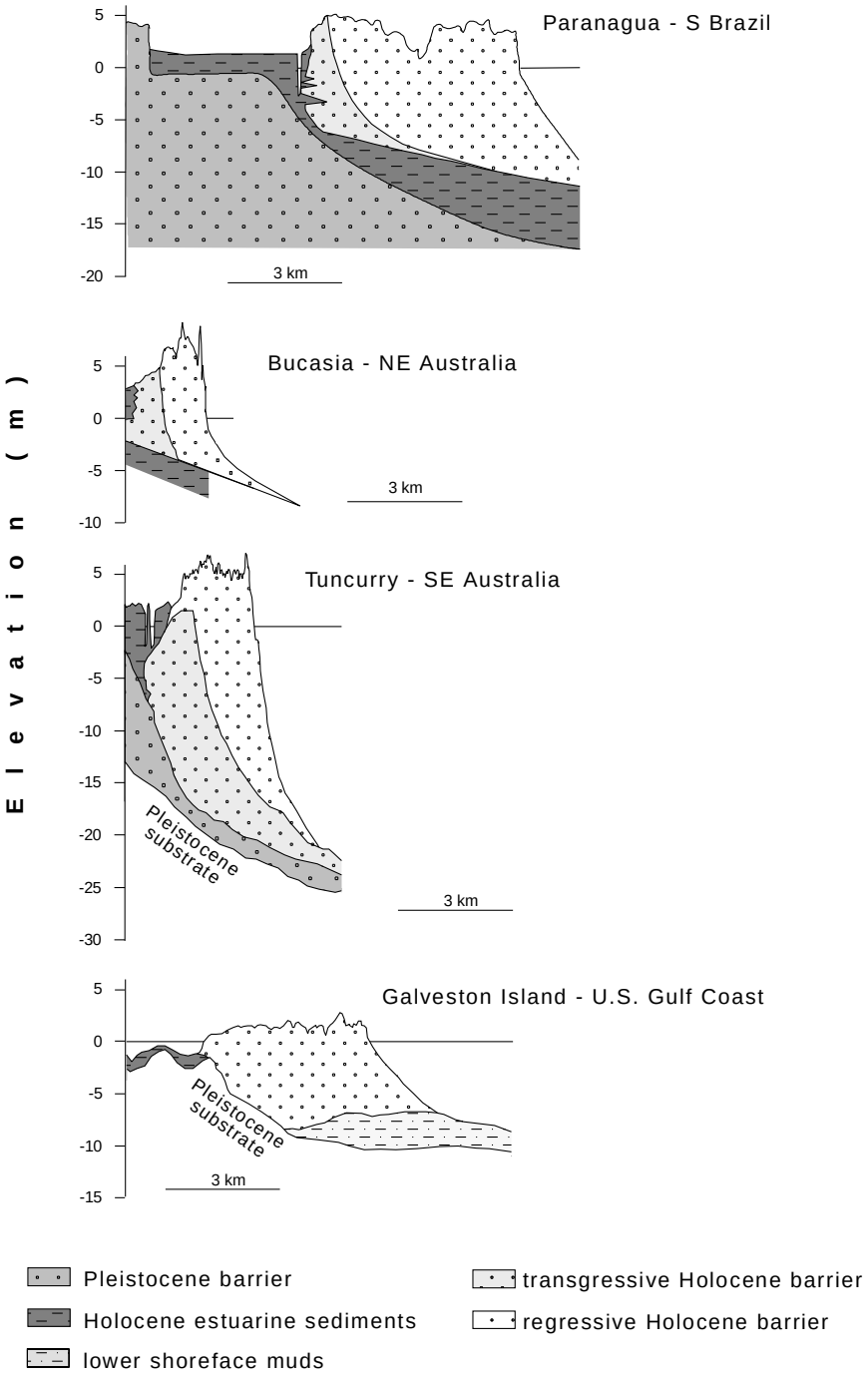

Fig. 11. Stratigraphic profile of regressive barriers (Bucasia modified after Masselink and Lessa, 1995; Tuncurry after Roy et al., 1995; Galveston Island after McCubbin, 1981).

Table 2
Average mean wave height and its standard deviation based on one year observation (Young and Olland, 1996), wave period, mean sediment diameter and approximate maximum depth of the wave surface of erosion (Hallermeier, 1981) for each barrier. Second line in Tuncurry refers to measured offshore wave data at Crowdy Head between 1895 and 1997 (source: Manly Hydraulics Laboratory, New South Wales Department of Public Works and Services)

Barrier	H_{avg} (m)	H_{std} (σ) (m)	T_{avg} (s)	D (mm)	d_i (m)
Paranaguá	1.35	0.19	10	0.25	36
Tuncurry	2.23	0.28	10[a]	0.25[b]	60
	1.63	0.60	7.9	0.25	32
Bucasia	1.33	0.28	7[c]	0.25[d]	8
Galvestone	1.23	0.18	8[e]	0.18[f]	31

[a] Short (1984).
[b] Roy et al. (1995).
[c] BPA (1986).
[d] Masselink and Lessa, 1995.
[e] National Data Buoy Center (http://scaboard.ndbc.noaa.gov).
[f] McCubbin (1981).

coast ($H \cong 1.0$ m and $T \cong 10$ s), and as such the toe of the shoreface would be positioned between these two extremes. However, no offshore data is available to determine the depth. One way to circumvent the lack of data is to estimate the depth of a paleo-shoreface, and assume that the wave climate and sediment budget have not changed considerably in the last few thousand years. The depth of a paleo-shoreface, given by the contact between the barrier and estuarine deposits in Rc#7 (Fig. 9b), appears to be 10 m below the present MSL, or about 12–13 m below the paleo MSL.

Hallermeier (1981) suggested that the limiting depth of an active beach profile under a changing sea level (ravinement surface or regressive wave surface of erosion) is similar to the maximum depth of sediment entrainment (d_i), which is a function of the mean significant wave height (H_s) and its standard deviation (σ), as well as the mean significant wave period (T_s) and mean sediment diameter (D) ($d_i = (H_s - 0.3\sigma)T_s(g/5000D)^{0.5}$). Based on the existing wave measurements for the study area (Table 1), d_i is estimated as 70 m, which is much deeper than the stratigraphic evidence suggests. Radar wave measurements (Young and Olland, 1996) (Table 2) for the area point to a shallower maximum depth of wave entrainment, which is still deeper than that implied by the stratigraphy.

Table 2 also lists the variables related to the other three sites and, with the exception of Bucasia, the estimated d_i values are also deeper than the depth of wave erosion suggested by the stratigraphy, implying that profile calculations based on this equation can be overestimated.

5.3. Longshore sediment budget/flux

In a longshore (S–N) direction the contact between barrier and paleo-estuarine deposits beneath the Holocene barrier deepens northwards, from an average elevation of −8 m in the center and south of the barrier to an average elevation of −13 m close to the estuary (including Rc#11–#22) (Fig. 5). The transgressive paleo-estuarine deposit is actually completely absent in the 30 m of Rc#11and #15, indicating that at these sites the deposit might have been completely removed, or have never formed. It appears that erosion of the transgressive paleo-estuarine sequence at the northern end of the barrier may have been caused by a tidal diastem, as the Paranaguá Bay entrance appears to have migrated northwards simultaneously with coastal progradation.

A longshore, north-bound barrier growth since the last highstand (as implied by the ^{14}C dating at exposure J, Fig. 7) is suggested by the presence of sedimentary deposits associated with a NW–SE orientated tidal channel 7 km south of the present Paranaguá Bay entrance location. The evidence is: (i) current megaripples in the exposures A, J and I (Fig. 7) indicating strong tidal flows and net sediment transport direction to the NW (see section 4.2); (ii) the apparent facies succession (tidal channel, upper shoreface, nearshore and beach) in vibro-core #18 (Fig. 6) and exposure A (Fig. 7); and (iii) the existence of open marine shell species within coarse estuarine deposits beneath Rasa da Cotinga Island (Fig. 1, Lessa et al., 1998), a location far from the area possibly influenced by present strong tidal flows. Therefore, deeper transgressive paleo-estuarine deposits observed in the Rc-cores #12, #13 and #16–#23 (Fig. 4) might have been eroded by a tidal diastem as the coastline prograded east- and northwards.

The likely occurrence of longshore barrier growth since the last highstand means that there has been a somewhat continuous, and possibly varying longshore supply of sand for at least 5000 years. Based on the

elevation of the sedimentary structures in vibro-cores #5, #7 and #8, and assuming that the beach-to-nearshore transition occurs around mean low water level (Short 1984), it appears that the seaward half (2500 m) of the Holocene barrier (Fig.9b) prograded with only 0.5 m of sea level fall, or within the last 1000 years as suggested by paleo-sea level indicators (Angulo et al., 1996; Angulo and Lessa, 1997). If this is correct, shoreline progradation was a result of sediment drift imbalances in the order of $+7.5\ m^3/m$ per length of the beach/year. This volume would not correspond to anything larger than 0.002% of the estimated net annual sediment flux (see description of the study area), and would be in agreement with values of positive drift imbalances given by Cowell et al. (1995) when simulating shoreline progradation in southeastern Australia.

This apparently swift coastal progradation suggests that a major influx of sediment occurred recently. The last 3 km at the northern end of the barrier, with an area of $15\ km^2$, is at least 1 m lower than places further south (Fig. 4, inset). This lower elevation may be ascribed to shoreline progradation under the influence of an ebb tidal delta, which dampens the wave height, or be associated with a more recent progradation, under conditions of relatively lower sea level. It is not possible to say whether an ebb tidal delta already existed when this part of the coast was accreting, but assuming it was not (flood dominance is suggested for the estuary around the high-stand—see Lessa et al., 1999) a volume of about $585 \times 10^6\ m^3$ of sand would have been deposited in the very late Holocene (given an average barrier thickness of 13 m in this area—Fig. 5). This volume is about one quarter of the total Holocene barrier volume, calculated at $1.87 \times 10^9\ m^3$ (assuming an overall average barrier thickness of 10 m).

There are two major estuaries to the south of the Paranaguá barrier, namely the Guaratuba Bay and São Francisco Bay estuaries (Fig. 12). Although information on these estuaries is scarce, they are largely still unfilled and, like the estuary of Paranaguá Bay, do not appear to yield sand size sediments to the coastal zone. The only fluvial sediment source south of Paranaguá would be the Itajaí River, 160 km away. The river is highly stratified (Schettini and Carvalho, 1996), and may only release sand size sediments into the coastal zone during floods (Ponçano and Gimenez, 1987). It discharges between two rocky headlands, in an area protected from the S–SW waves, and therefore is not very likely to contribute with a significant sediment volume to the littoral drift system. Hence, the only source of sand to the study area appears to be the erosion of the immediate coastline. The distribution of Holocene and Pleistocene barriers south of Paranaguá, with the −5, −10 and −20 m isobaths, is shown in Fig. 12 (Itajaí river is about 10 km south of Ponta do Vigia headland). It is observed that Holocene barriers are practically absent in the south of the area, where the Pleistocene barrier abuts the shore. The Holocene barriers become increasingly more prominent northwards, especially at the southern side of estuarine mouths, as would be expected considering a south–north littoral drift system.

Fig. 12 (inset) shows the variation in area of the Holocene barrier for every 5 km of the coast, pointing to an excessive larger area (and volume) of Holocene sediment accumulation in the Paranaguá sector. An inspection of the isobaths also show a clear trend of more voluminous sediment accretion to the north, especially if one observes the −5 and −10 m isobath. The evidence points to the existence of a littoral cell of sediment circulation, from the northern end of the State of Santa Catarina to the State of Paraná. The northward sediment transport does not seem to be interrupted along this coastline, since the estuaries exhibit well developed ebb tidal deltas, prone to sediment bypassing, and the few existing headlands are fronted by sea beds less than 10 m deep, thus within the zone of wave sediment reworking.

6. Conclusions

The morphostratigraphy of the Paranaguá coastal plain reveals the existence of extensive regressive deposits built at least after the last two interglacials (120 000 and 5100 years B.P.). Reverse-circulation cores from the innermost sectors of the plain suggest that barrier deposits are around 20 m thick, overlying transgressive estuary deposits that sit upon some 40 m of continental (fluvial and alluvial-fan) sediments. The Pleistocene barrier appears to form the substrate for the Holocene marine sedimentation close to shore, where its thickness would be twice that of the Holocene barrier.

Estuarine sedimentation shows contrasting textural characteristics underneath the present shoreline and

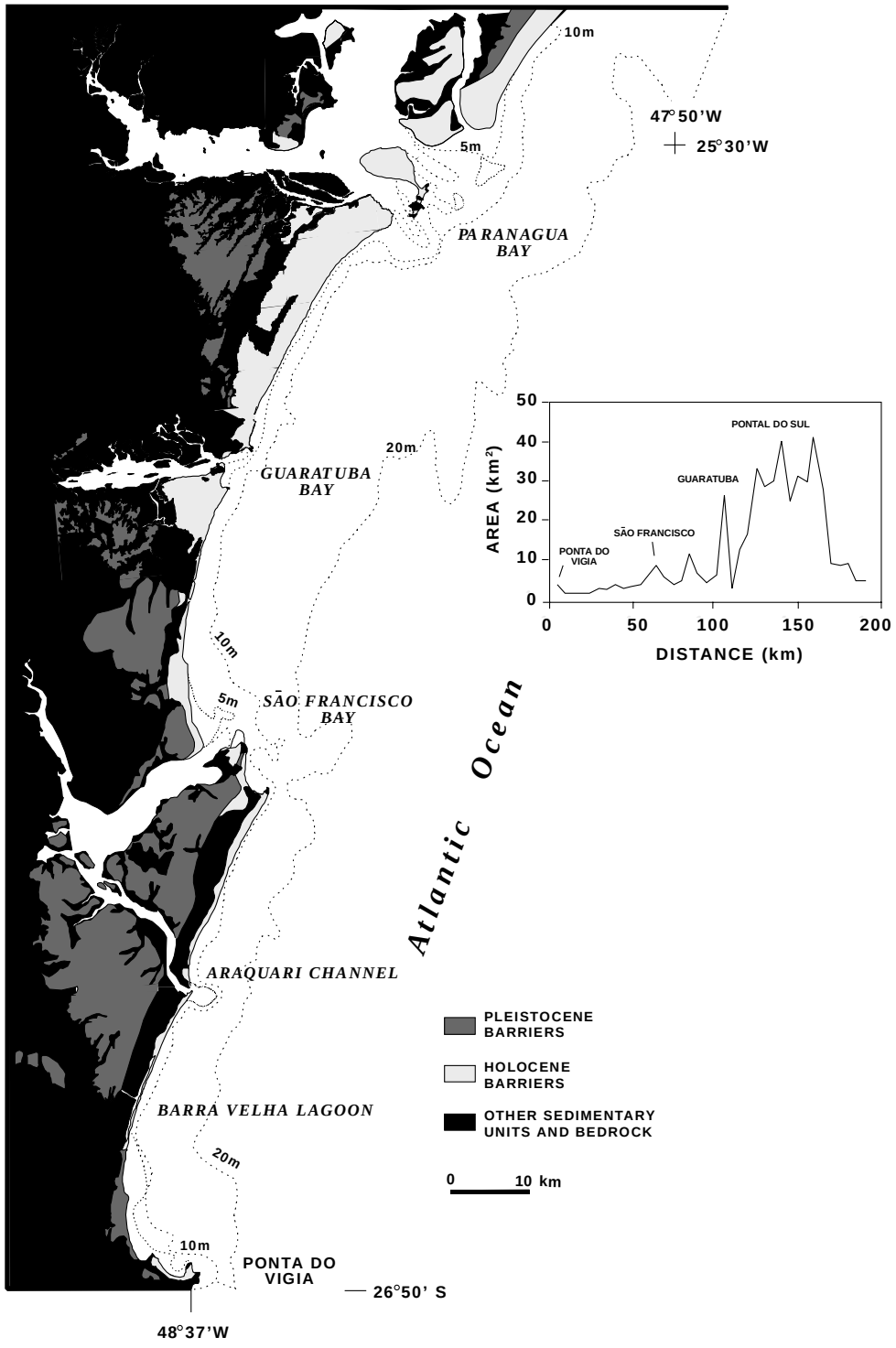

Fig. 12. Distribution of Pleistocene and Holocene barriers and the bathymetric contour close to the shoreline along the coastline to the south of Paranaguá coastal plain. Note the southward narrowing of the Holocene barriers and the bathymetric lines. The inset shows the area of the Holocene barrier at every 5 km along the coast.

behind the barrier. Muddy sediments beneath the present shoreline indicate a much calmer environment than that associated with the coarse estuarine channel deposits that interfinger with the overwash facies at the rear of the barrier. This change in the back-barrier environment is possibly related to reduced accommodation space associated with a steepening substrate profile, which ended up squeezing the estuary at a certain point during the transgression. The estuary, however, appears to have been able to clear its way through both barriers, eroding all the transgressive sequence at the northern side of the Holocene barrier. Complete barrier encroachment occurred in Superagui Island, the second-next barrier to the north, probably due to the absence of sizeable stream flows.

The elevation of the Pleistocene barrier, as well as the elevation of the open marine sedimentary facies in the Pleistocene and Holocene barriers, suggests that the sea level associated with the later stages of the Pleistocene barrier progradation was lower than the Holocene sea level maximum. The facies' elevation also suggest a later phase of more rapid progradation, when half of the present barrier prograded with about 0.5 m of sea level fall, or in the last one thousand years or so. Coastal progradation and longshore barrier growth might have occurred all along the regressive barrier phase. The location of the estuary mouth 10 km to the south at around the highstand, as indicated by flood tidal delta deposits dated at 4300 ± 70 years B.P., point to a continuous S–N process of longhshore sediment feeding. Sediment sources appear to be associated with the erosion of barrier deposits to the south of the area.

The transition between barrier and paleo-estuarine sediments indicates the depth of the shoreface profile which actually translated with barrier progradation. Although carried out with a very limited data set, comparison of the contact elevation between regressive and transgressive facies in four barriers suggests that the depth of effective wave erosion during the translation of the shoreface profile could be shallower than that indicated by the equation proposed by Hallermeier (1981).

Acknowledgements

We would like to thank T. Janner Engenharia and Solotécnica for providing copies of the core logs performed on the coastal plain. Many thanks also go to Carlos Soares, Célia Riesemberg, Alberto Neto, Cláudio Silva, Fernando Pilatti, Marcelo Lamur and Abraão for helping with the vibro-cores and cleaning of the many exposures along the creek banks. We are also thankful to Mark Kulmar (Manly Hydraulics Lab.) for kindly providing wave data from Crowdy Head. The quality of the manuscript was greatly improved with comments made by Dr Sérgio Dillemburg, Dr Peter Roy and an anonymous referee.

References

Angulo, R.J., 1992. Geologia da Planície Costeira do Estado do Paraná. Unpublished PhD Dissertation, Geoscience Institute, University of São Paulo, Brasil, p. 334.

Angulo, R.J., 1995. Caracterização e reavaliação da Formação Alexandra (Terciário) e de sedimentos continentais associados a vertentes no litoral do Estado do Paraná Brasil. An. Acad. Bras. Ciên. Rio de Janeiro 67 (4), 443–463.

Angulo, R.J., 1995. Feições deposicionais associadas às desembocaduras dos complexos estuarinos da costa paranaense. Proc. 5th Cong. Braz. Ass. of Quat. Studies (ABEQUA), Niterói, Brazil, pp. 58–64.

Angulo, R.J., Lessa, G.C., 1997. The Brazilian sea level curves: a critical review with emphasis on the curves from Paranaguá and Cananéia regions. Mar. Geol. 140, 141–166.

Angulo, R.J., Suguio, K., 1995. Re-evaluation of the Holocene sea-level maxima for the state of Paraná, Brazil. Paleogeol. Paleoclimol. Paleontol. 113, 385–393.

Angulo, R.J., Giannini, P.C.F., Suguio, K., Pessedna, L.C.F., 1996. Variações relativas do nível médio do mar nos últimos 5500 anos na região de Laguna-Imbituba (Santa Catarina), com base em datações radiocarbônicas de tubos de vermitídeos. Proc. 39th Braz. Geol. Cong., Salvador, Brazil, pp. 281–284.

Angulo, R.J., Souza, M.C., Araújo, A.D., Pessenda, L.C.R., Odreski, L.L.R., Lamour, M.R., Carrilho, J.C., Nadal, C.A., 1999. Fácies sedimentares de uma barreira regressiva holocênica na planície costeira de Praia de Leste. Estado do Paraná. Proc. Seventh Cong. Braz. Ass. of Quat. Studies (ABEQUA), Porto Seguro, Brazil (in press).

Araujo, A.D., Lessa, G.C., 1996. Nível médio do mar e estruturas praias: uma contribuição ao estudo paleogeográfico da planície costeira Paranaense. Proc. 39th Braz. Geol. Cong., Salvador, Brazil, pp. 237–240.

APPA, 1994—Administração dos Portos de Paranaguá e Antonina, 1994. Resumo dos serviços de dragagem de manutenção do canal de acesso ao porto de Paranaguá, p. 3 (unpublished report).

Barreto, A.M.F., Angulo, R.J., Tatumi, S.H., Watanabe, S., Ayta, W.E.F., 1999. Datações por termoluminescência (TL) de sedimentos da planície costeira de Paranaguá. Estado do Paraná. Proc. Seventh Cong. Braz. Assoc. Quat. Studies (ABEQUA), Porto Seguro, Brazil (in press).

Bigarella, J.J., 1946. Contribuição ao estudo da planície litorânea do Estado do Paraná. Arq. Biol. Técn. 1, 75–111.

Bigarella, J.J., 1965. Sand-ridges structures from Paraná coastal plain. Mar. Geol. 3, 269–278.

Bigarella, J.J., Becker, R.D., Matos, D.J., Werner, A., 1978. A Serra do Mar e a Porção Oriental do Estado do Paraná. Secretaria de Estado do Planejamento, Governo do Paraná, p. 248.

B.P.A.—Beach Protection Authority of Queensland, 1986. Wave Data Recording Programme: Mackay Region. Beach Protection Authority of Queensland (unpublished).

Cowell, P.J., Roy, P.S., Jones, R.A., 1995. Simulation of large-scale coastal change using a morphological behaviour model. Mar. Geol. 126, 45–61.

Curray, J.R., Emmel, F.J., Crampton, P.J.S., 1969. In: Castanares, A.A., Phleger, F.B. (Eds.), Holocene history of strandplain, lagoonal coasts, Nayarit, Mexico Coastal Lagoons, a Symposium, Universidad Nacional Autonoma, Mexico, pp. 63–100.

Davies, D.K., Ethridge, F.G., Berg, R.R., 1971. Recognition of barriers environments. Am. Assoc. Pet. Bull. 55 (4), 551–565.

Dominguez, J.M.L., Wanless, H.R., 1991. Facies architecture of a falling sea-level strandplain, Doce River coast, Brazil. Spec. Pub. Int. Ass. Sedimentologists 14, 259–281.

Domingues, J.M.L., Bittencourt, A.C.S.P., Martin, L., 1992. Controls on Quaternary coastal evolution of the east–northeastern coast of Brazil: roles of sea-level history, trade winds and climate. Sed. Geol. 80, 213–232.

Gagan, M.K., Johnson, D.P., Crowley, G.M., 1994. Sea level control of stacked late Quaternary sequences, central Great Barrier Reef. Sedimentology 41, 329–351.

Galehouse, J.S., 1971. Point counting. In: Carver, R.E. (Ed.), Procedures in Sedimentary Petrology, Wiley, New York, pp. 385–407.

Hallermeier, R.J., 1981. A profile zonation for seasonal sand beaches from wave climate. Coast. Engng. 4, 253–277.

Harari, J., de Camargo, R., 1994. Simulação da propagação das nove principais componentes de maré na plataforma sudeste brasileira através de modelo numérico hidrodinâmico. Boletim Instituto Oceanográfico—USP 42 (1), 35–54.

Helland-Hansen, W., Martinsen, O.J., 1996. Shoreline trajectories and sequences: description of variable depositional-dip scenarios. J. Sed. Res. 66 (4), 670–688.

Kraft, J.C., Chrzastowski, M.J., 1985. Costal stratigraphy sequences. In: Davis Jr., R.A. (Ed.), Coastal Sedimentary Environments, Springer, New York, pp. 625–664.

Kraft, J.C., John, C.J., Marx, P.R., 1981. Clastic depositonal strata in a transgressive coastal environment: Holocene Epoch. Northeast. Geol. 3 (3/4), 268–277.

Lima, M.R., e Angulo, R.J., 1990. Descoberta de microflora em um nível linhítico da Formação Alexandra, Terciário do Estado do Paraná Brasil. An. Acad. Bras. Ciên. 62 (4), 357–371.

Lessa, G.C., Angulo, R.J., 1995. A framework for the stratigraphy and evolution of the Paranaguá coastal plain—Paraná, Brazil. Proc. Fifth Cong. Braz. Ass. of Quat. Studies (ABEQUA), Niterói, Brazil, pp. 92–98.

Lessa, G.C., Angulo, R.J., 1998. Oscillations or not oscillations: that is the question—Reply. Mar. Geol. 150, 189–196.

Lessa, G.C., Meyers, S.D., Marone, E., 1999. Holocene stratigraphy in Paranaguá Bay estuary, south Brazil. J. Sed. Res. 68 (6), 1060–1076.

Maack, R., 1949. Espessura e sequência dos sedimentos quaternários no litoral do Estado do Paraná. Arquivos de Biologia e Tecnologia 44 (19), 271–295.

Martin, L., Suguio, K., Flexor, J.M., Azevedo, A.E.G., 1988. Mapa Geológico do Quaternário Costeiro dos Estados do Paraná e Santa Catarina. Série Geológica DNPM 28, 40.

Masselink, G., Lessa, G.C., 1995. Barrier stratigraphy on the macrotidal central Queensland coastline. Aust. J. Coast. Res. 11 (2), 454–477.

McCubbin, D.G., 1981. Barrier-island and strand plain facies. In: Scholle, P.A., Spearing, D. (Eds.), Sandstone Depositional Environments, The American Association of Petroleum Geologists, Tulsa, Oklahoma, USA, pp. 247–280.

Mio, E., Giannini, P.C.F., 1997. Variação de minerais pesados transversal à planície costeira de Peruípe-Itanhaém, SP. Proc. Sixth Cong. Braz. Assoc. Quatern. Stud. (ABEQUA), Curitiba, pp. 109–113.

Murakoshi, N., Masuda, F., 1992. Estuarine, barrier-island to strandplain sequence and related ravinement surface developed during the last interglacial in the paleo-Tokyo Bay, Japan. Sed. Geol. 80, 167–184.

Ponçano, W.L., Gimenez, A.F., 1987. Reconhecimento sedimentológico do estuário do rio Itajaí-Açu. Ver. Bras. de Geoc. 17 (1), 33–41.

PORTOBRAS, 1983. Campanha de medicoes de ondas em Paranagua - PR (período 21/08/1982 a 21/01/1983). Divisão de Apoio Técnico e Cientifico (DIATEC), Instituto de Pesquisas Hidroviárias (INPH), Relatório INPH 34/83, Rio de Janeiro, p. 23.

Posamentier, H.W., Allen, G.P., James, D.P., 1992. High resolution sequence stratigraphy—the East Coulee delta. Alberta. J. Sed. Pet. 62 (2), 310–317.

Riverau, J.C., Fuck, R.A., Muratori, A., Trein, E., 1969. Paranaguá, folha geológica. Comissão Carta geológica do Paraná (escala 1:70.000).

Roy, P., Cowell, P.J., Ferland, M.A., Thom, B.G., 1995. Wave dominated coasts. In: Carter, R.W.G., Woodroffe, C.D. (Eds.), Coastal Evolution, Cambridge University Press, Cambridge, pp. 121–186.

Sayão, O.J., 1989. Littoral drift along some beahes in Brazil. In: Magoon, O.T., Converse, H., Miner, D., Tobin, L.T., Clark, D. (Eds.), Proc. Sixth Symp. Coast. Ocean Manag., Charleston, USA, vol. 4. AmericanSociety of Civil Engineers, pp. 3638–3746.

Schettini, C.A.F., Carvalho, J.L.B., 1996. Avaliação preliminar do transporte residual de material em suspensão no estuário do Itajaí-Açu SC. Proc, 39th Braz. Geol. Cong., Salvador, Brazil 5, 245–248.

Short, A.D., 1984. Beach and nearshore facies: southeast Australia. Mar. Geol. 60, 261–282.

Soares, C.R., Paranhos Filho, A.C., Souza, M.C., Branco, J.C., Fabianovicz, R., Prazeres Filho, H.J., Kogut, J.S., 1994. Variações da linha de costa no balneário de Pontal do Sul entre e: um balanço sedimentar. Bol. Paranaense Geoc. Paranhos Filho 42, 161–171.

Suguio, K., Martin, L., 1976. Brazilian coastline quaternary formations the States of São Paulo and Bahia littoral zone evolutive schemes. An. Acad. Bras. Ciênc. 48, 325–334.

Suguio, K., Martin, L., Bittencourt, A.C.S.P., Domingues, J.M.L., Flexor, J.M., Azevedo, A.E.G., 1985. Flutuações do nível relativo do mar durante o Quaternário Superior ao longo do litoral brasileiro e suas implicações na sedimentação costeira. Rev. Bras. Geoc. 15, 273–286.

Swift, D.J.P., 1976. Coastal Sedimentation. In: Stanley, D.J., Swift, D.J.P. (Eds.), Marine Sediment Transport and Environmental Management, Wiley, New York, pp. 255–310.

Tessler, M.G., 1988. Dinâmica Sedimentar Quaternária no Litoral Paulista. Unpublished PhD Dissertation, Geoscience Institute, University of São Paulo, Brasil, p. 277.

Villwock, J.A., Tomazelli, L.J., Loss, E.L., Dehnhardt, E.A., Horn, N.O., Bachi, F.A., Dehnhardt, B.A., 1986. In: Rabassa, J. (Ed.), Geology of Rio Grande do Sul coastal province, vol. 4. Quat. South Am. Antartic Peninsula, pp. 79–97.

Young, I.R., Olland, G.J., 1996. Atlas of the Ocean: Wind and Wave Climate, Interactive Series, Pergamon and Elsevier, Amsterdam.